PNAS RESEARCH ARTICLE | PLANT BIOLOGY
EARTH, ATMOSPHERIC, AND PLANETARY SCIENCES

Extreme triple oxygen isotope fractionation in *Equisetum*

Zachary Sharp[a,1], Jordan Wostbrock[b], Anthony Gargano[c], Vincent Hare[d], Jessica Johnson[a,2], Thure Cerling[e,f], Payal Banerjee[a], Catherine Peshek[a], Cloe Knutson[a], Lauren Hartzell[a], Erick Cano[g], Elena Stiles[h,3], Kelley R. Bassett[i,3], Kira Holland[j,3], Michael H. Dowd[k,3], Jarunetr (Nadia) Sae-Lim[l,3], Teresa Dominguez[m,3], Dalton Bryant[m,3], Eduardo Di Marcantonio[n,3], Jensen Wainwright[o,3], Maxwell Horsford[p,3], Paul Botté[q,3], Catherine Gagnon[r,3], Paula J. Rudall[s], and James Ehleringer[f]

Affiliations are included on p. 7.

Edited by Donald Canfield, Syddansk Universitet, Odense M., Denmark; received April 13, 2025; accepted September 30, 2025

Triple oxygen isotope values of xylem water were measured along the length of smooth horsetail stems (*Equisetum laevigatum*). Extreme isotope enrichment is observed moving from base to stem tip. $\delta^{18}O$ values range from −8.3‰ at the base to 82.6‰ at the tip. $\Delta'^{17}O$ values range from 0 to −1,797 per meg. The $\delta^{18}O$ and $\Delta'^{17}O$ values are the most extreme measured for any terrestrial material and expand the known range of $\Delta'^{17}O$ values by fivefold for mass-dependent fractionation on Earth. The extreme isotope enrichments are explained using a hybrid evaporation/chain-of-lakes model, allowing us to refine the leaf respiration coefficient to $\theta_k = 0.511 \pm 0.001$. This new value is required to explain the low $\Delta'^{17}O$ values previously measured in desert plants and animals and is critical when using fossil samples for paleoclimate reconstruction. Coexisting phytoliths and stem water were also measured. The $1000ln^{18}\alpha_{silica\text{-}water}$ value at the plant base (35.89‰) appears to be in isotopic equilibrium, with far smaller fractionations of 10.3‰ near the tip. The smaller fractionations at higher levels are explained by continual silica deposition as the plant elongates and the $\delta^{18}O$ values of each segment become higher. The overall integrated phytolith value is a combination of early and late silica growth. The $\Delta'^{17}O_{silica} - \Delta'^{17}O_{water}$ values are not in equilibrium, explained by a kinetic isotope effect, with a λ value of 0.5205 vs. 0.5244 for equilibrium. Phytolith isotope values may lead to erroneous interpretations for paleoclimate reconstruction.

triple oxygen isotopes | extreme isotope fractionation | plant physiology | phytolith isotope chemistry | paleoclimatology

Significance

Isotopic enrichment in *Equisetum* is extreme due to evaporative water loss along the entire plant stem. The *Equisetum* data extend the known oxygen isotope range of samples from Earth and our entire solar system by a factor of five. Bulk oxygen isotope values of phytoliths (amorphous silica) are not representative of xylem water, so that caution is needed when interpreting phytolith isotope data for paleoclimate reconstruction. Existing models for plant water and by extension animal water isotope data can explain the extreme fractionation that occurs in arid environments using a revised triple oxygen isotope diffusion fractionation factor θk = 0.511 ± 0.001. This new value explains low $\Delta'^{17}O$ values of natural materials, particularly in arid environments.

Transfer of water from soil into the atmosphere via plant transpiration accounts for up to 80% of water loss from land (1). In a simple sense, water is taken up by the roots, transferred upward by the stems, and either combined with carbon dioxide to form carbohydrates during photosynthesis, or released to the atmosphere through the stomata in the green leaves and stems. It is generally accepted that water uptake by roots occurs with negligible isotopic fractionation (2). Similarly, water movement through xylem occurs in a partially closed system absent of any isotope fractionation. In contrast, there is a large isotope fractionation across plant tissues as water is lost as water vapor through the stomata (e.g., ref. 3). In terms of equilibrium mass balance, the product of the water flux and isotopic composition of water vapor diffusing though the stomata must be equal to the input in the root system (4). Because of the preferential loss of light isotopes in water vapor, the water in aerial organs becomes heavier than that taken up by the roots. To a first approximation, water approaches isotopic steady state (5, 6) and can be modeled as such (7).

Apart from small fraction of water used in photosynthetic reactions, the majority of water loss from leaves or green stems occurs through stomata. Isotope fractionation occurs because the vapor pressure of $H_2{}^{18}O$ is less than $H_2{}^{16}O$, such that evaporation tends to favor the light isotopologs (3, 4, 8). The isotope effect is primarily controlled by the difference in the partial pressures of water within the leaf (e_i) and at the leaf surface (e_s). While a constant isotopic composition of leaf water is expected in most leaves, long, linear leaf blades, such as grasses, have more enrichment toward the leaf tip. Here, transpiration occurs with diffusive isotopic exchange between evaporating surfaces and xylem along the entire leaf length (7, 9, 10). In grasses, there can be a 20‰ increase in the oxygen isotope ratio of leaf water from the leaf base to its tip (9). The magnitude of isotopic enrichment is greater under conditions of lower relative humidity.

Equisetum, commonly known as horsetails, belongs to one of the oldest known vascular plant lineages, dating back to the Devonian period (11, 12), where ancestor heights reached 15 to 20 m (13, 14). Modern *Equisetum* species range in height from ~12.9 cm (*Equisetum scirpoides*) to 8 m (*Equisetum giganteum* and *Equisetum myriochaetum*) (12).

Author contributions: Z.S., J. Wostbrock, T.C., and J.E. designed research; Z.S., J. Wostbrock, A.G., and J.J. performed research; Z.S., A.G., V.H., P. Banerjee, C.P., C.K., L.H., E.C., E.S., K.R.B., K.H., M.H.D., J.N.S.-L., T.D., D.B., E.D.M., J. Wainwright, M.H., P. Botté, C.G., P.J.R., and J.E. analyzed data; and Z.S., J. Wostbrock, P.J.R., and J.E. wrote the paper.

The authors declare no competing interest.

This article is a PNAS Direct Submission.

[1]To whom correspondence may be addressed. Email: zsharp@unm.edu.

[2]Present address: School of Science, Math, and Engineering, Central New Mexico Community College, Albuquerque NM 87106.

[3]Isocamp team member.

This article contains supporting information online at https://www.pnas.org/lookup/suppl/doi:10.1073/pnas.2507455122/-/DCSupplemental.

Published October 28, 2025.

The morphology and anatomy of *Equisetum* are unique among living land plants; the upright aerial stems grow as a series of jointed segments (Fig. 1), each of which has the capacity to transpire (15). Each segment contains rows of stomata along the entire length of the stem (16–18) with each segment thought to have equivalent conductance to water loss (15, 19). The simple cylindrical geometry of *Equisetum* combined with over a million stomata along the meter-long stalk (Fig. 1) manifests as an extreme distillation column that can be modeled to determine the fundamental isotope fractionation parameters for transpiration.

In this contribution, we measured the triple oxygen isotope composition of stem water and silica phytoliths in *Equisetum* along the full length of the jointed and segmented stem in order to estimate the isotope effects during this extreme "distillation" process. Three samples of horsetail (*Equisetum laevigatum*) collected in different years (2021, 2023, and 2024) were analyzed and found to have nearly identical isotope profiles (Table 1). Samples were collected 100 m west of the Rio Grande in Albuquerque, NM. The field site is in the cottonwood forest that borders the river. It is partially shaded with an average summer relative humidity of ~25% (see *SI Appendix* for further details).

Results

Xylem Water. The $\delta^{18}O$ and $\delta^{17}O$ values of *Equisetum* stem water increase regularly with distance from the base to the tip of the aerial stem (Fig. 2 and Table 1). The $\delta^{18}O$ values increase from the ambient soil water values of ~−8‰ (VSMOW) at the ground surface to 82‰ at the tip. The $\Delta'^{17}O$ values of stem water decrease from 20 to 30 per meg at the base to −1,797 per meg at the stem tip. There is a regular change within individual nodes as well as between nodes, suggesting that the nodes do not present a significant restriction to water transport. The lowest $\Delta'^{17}O$ values are a factor of five more negative than anything previously measured on Earth (20–23), explained by the extreme kinetic fractionation associated with continual water loss along the plant stem.

To a first order, the stem water of *Equisetum* can be modeled as simple Rayleigh fractionation, where $R_{liquid}/R_{initial\ liquid} = F^{(\alpha-1)}$. In the case of *Equisetum*, Rayleigh fractionation is akin to continuous removal of vapor from the plant stem with a fixed isotope fractionation. Each isolated parcel of water moves upward through the stem, continuously losing isotopically light water through the stomata. In the Rayleigh equation, R is the ratio of the heavy to light isotope (i.e., $^{17}O/^{16}O$ or $^{18}O/^{16}O$), F is the fraction of water remaining in the sample, and α is the isotope fractionation factor between the water remaining in the leaf relative to the water vapor that is lost by transpiration, given by $\alpha_{vapor-water} = \frac{R_{vapor}}{R_{water}}$. (All isotope equations in this paper are equally valid for $^{18}O/^{16}O$ and $^{17}O/^{16}O$. The α values for $^{17}O/^{16}O$ fractionation are given by $^{17O/16O}\alpha = (^{18O/16O}\alpha)^{\theta}$. θ values are determined experimentally or theoretically (e.g., refs. 25–27). The common delta notation is

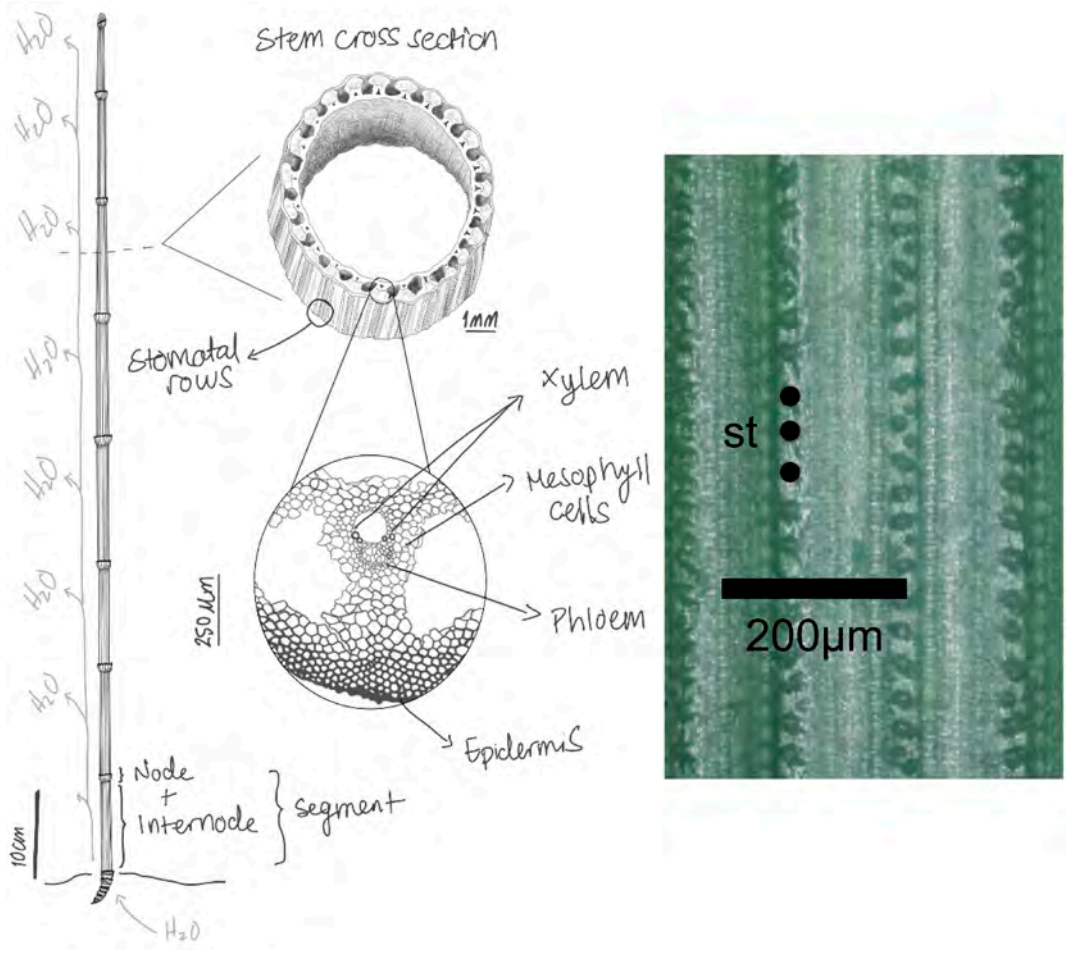

Fig. 1. Longitudinal and cross-section sketch of an *Equisetum* stem. External water loss (transpiration) occurs through stomatal rows in each of the photosynthetic stem segments. While xylem cells and carinal canals supply water to cells within a stem segment, the limited number of mesophyll cells between the evaporating surfaces and xylem (*Inset*) provides a mechanism for back diffusion between isotopically enriched evaporating cells and xylem. Photo shows the size and regular distribution of stomata (st). Illustration by E. Stiles.

Table 1. Triple oxygen isotope composition of stem segment water, phytoliths, and atmospheric water vapor relative to Vienna Standard Mean Ocean Water (VSMOW)

Segment_ number	Mid-segment distance (cm)	$\delta^{17}O$ ‰ VSMOW	$\delta^{18}O$‰ VSMOW	$\Delta'^{17}O$ permeg	$\delta^{17}O$‰ VSMOW	$\delta^{18}O$‰ VSMOW	$\Delta'^{17}O$ permeg
			Stem water			Phytolith	
				Sample 1 (2024)			
1	2	−4.41	−8.34	0			
2	7	−3.95	−7.45	−7			
3	14	−3.03	−5.71	−11			
4.4	23.5	−1.42	−2.63	−31			
4.8	27	−0.24	−0.37	−50			
5	31.5	0.01	0.16	−77			
5.5	36.5	1.17	2.36	−80			
7	55.5	3.05	6.04	−135			
8	71.25	8.36	16.30	−208			
9	83	12.22	23.80	−270			
10	95	16.38	32.12	−446			
11	106	20.92	41.21	−621			
12	115.5	24.62	48.44	−660			
13	124.5	29.50	58.32	−852			
14	132.75	35.56	70.85	−1,200			
15	139.25	40.90	82.55	−1,797			
				Sample 2 (2023)			
4	n.d.	−0.28	−0.58	29			
8		8.10	15.63	−119			
12		21.14	41.12	−357			
14		28.70	56.16	−548			
19		45.73	91.84	−1,674			
				Sample 3 (2021)			
1	2	−6.37	−12.10	34	−12.29	24.00	−232
7	30	12.30	24.40	−433	20.64	40.60	−369
9	39	19.62	39.30	−735	25.26	50.10	−555
				Water vapor in air (2024)			
		−10.09	−19.21	56			

related to R by $\delta = (R_{sample}/R_{standard} - 1) \times 1{,}000$ in per mil notation. $\Delta'^{17}O$ is given by $\delta'^{17}O - 0.528 \times \delta'^{18}O$). Using an α value of 0.9727 based on diffusion rates of $H_2{}^{18}O$ and $H_2{}^{16}O$ in dry nitrogen (25), Rayleigh fractionation results in an imperfect fit to the data (Fig. 2). This is due in part to not considering the contribution of back-diffusion of atmospheric H_2O through the stomata and dispersion of water within the xylem.

A better model involves a more complete treatment of leaf transpiration related to the leaf–air vapor pressure difference and the atmospheric composition of the water vapor in air (4). The equation is given by ref. 8

$$R_l = \alpha^* \left(\alpha_k R_x \left(\frac{e_i - e_s}{e_i} \right) + \alpha_{kb} R_x \left(\frac{e_s - e_a}{e_i} \right) + R_a \left(\frac{e_a}{e_i} \right) \right). \quad [1]$$

R_x, R_l, and R_a are the $^{18}O/^{16}O$ ratio of the source water, leaf water (for *Equisetum*, this would be stem water), and water vapor in air, respectively. α* is the equilibrium water–water vapor fractionation at ambient temperature, α_k is the kinetic isotope fractionation across the stomata, α_{kb} is the kinetic fractionation across the boundary layer which is given by $\alpha_{kb} = \alpha_k{}^{2/3}$ (28). e_i, e_a, and e_s are the partial pressure of water vapor in the leaf intercellular air spaces, atmosphere, and leaf surface. Eq. **1** can be modified to include a chain-of-lakes model (29, 30) where the incoming stem water is partitioned between water vapor lost from the leaf and water that moves up into the next segment given by

$$R_x = x(R_a) + (1-x)(R_l). \quad [2]$$

x is the fraction of water vapor entering the segment that is lost by transpiration and can be approximated as being equal to $1/(1 + n_{segments\ remaining})$. For example, if we assume 20 equal segments, 1/(1 + 19), or 2% of the water entering the first segment is lost by transpiration. For the 5th segment 1/(1 + 15), or 6.25% is lost as water vapor. For the uppermost segment 1/(1 + 0) or 100% of the water is lost by transpiration. We consider the possibility that the amount

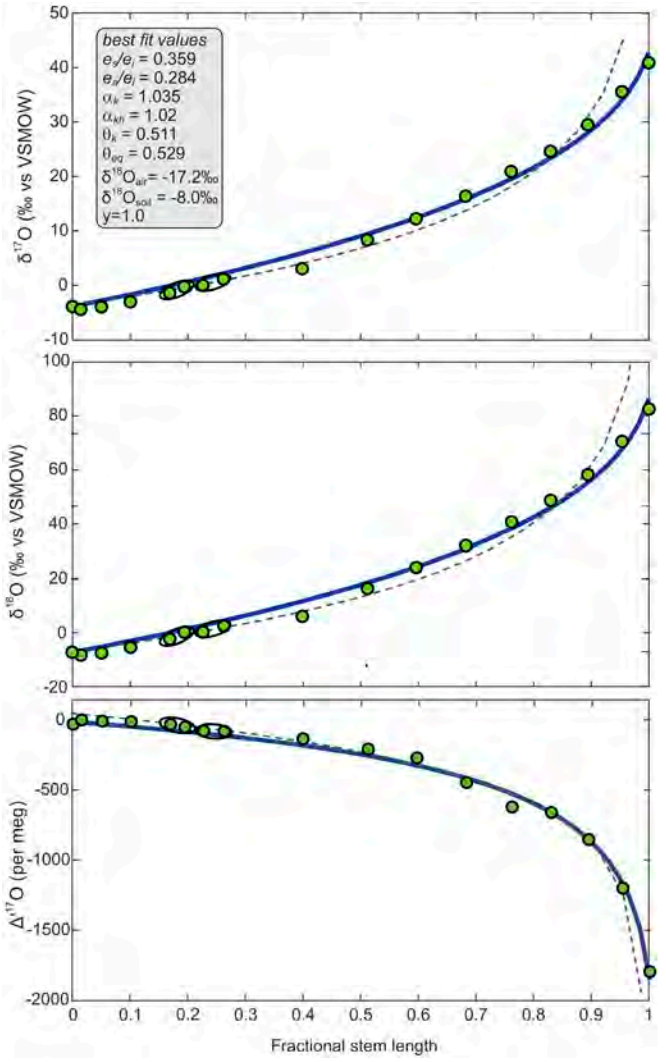

Fig. 2. $\delta^{18}O$, $\delta^{17}O$, and $\Delta'^{17}O$ along the length of an *Equisetum* stalk, fitted by Bayesian methods, to a model based on Eq. **4** (solid blue), with y = 1, and the following estimated parameters: e_i = 3.20 at 25.2 ± 1.0°C (1σ), e_s = 1.15 ± 0.36, e_a = 0.91 ± 0.10, α_{kh} = 1.020, and α_k = 1.035 (taken from 31), θ_k = 0.511 ± 0.001, θ_{eq} = 0.529 (taken from ref. 24), n = 57 ± 22. Light blue shaded areas indicate 95% prediction intervals of a model based on Eq. **4**, from the Bayesian analysis. Ellipses show samples from within the same segment. Rayleigh fit shown by the dashed line does not fit the data well. Total stem length = 142 cm. The best fit $\delta^{18}O_{soil}$ value was −8.0 ± 0.9‰, which implies a $\delta^{18}O_{water\ vapor}$ value of −17.2‰ (VSMOW), compared to a measured value of −19.0‰.

of water vapor lost at each segment varies regularly along the length of the stem, by raising the x value to an exponent such that

$$x = \left(\frac{1}{1 + n_{segments\ \ remaining}} \right)^{y}. \qquad [3]$$

The exponent y is varied to achieve a best fit to the measured data. Combining Eqs. **1** and **2** yields:

$$R_l = \frac{R_x + \frac{e_a R_a x}{e_i \alpha_k - e_s \alpha_k - e_a \alpha_{kh} + e_s \alpha_{kh}}}{1 - x + \frac{e_i x}{(e_i \alpha_k - e_s \alpha_k - e_a \alpha_{kh} + e_s \alpha_{kh})\alpha_{eq}}}, \qquad [4]$$

where x is given by Eq. **2**.

The measured data were fit to Eq. **4** for $\delta^{17}O$, $\delta^{18}O$, and $\Delta'^{17}O$ using a Bayesian parameter estimation (31) (Fig. 2 and *SI Appendix*). Best fits are obtained with: $\delta^{18}O_{water\ vapor}$ = −17.2‰ (VSMOW) compared to a measured value of −19.0‰, e_i = 3.20 at 25.2 °C (R_h = 100%), e_s = 1.15 ± 0.36 (1σ), e_a = 0.91 ± 0.10, α_{kh} = 1.02 and α_k = 1.035 (taken from ref. 32), θ_k = 0.511 ± 0.001, θ_{eq} = 0.529 (24), n = 57 ± 22, y = 1. The trends in $\delta^{17}O$ and $\delta^{18}O$ are captured by Eq. **4**, showing the reduction in curvature at higher delta values, and demonstrating the back-diffusion from the air into the stems. The θ_k value is at the low end of some previous estimates (26, 32), but in good agreement with others (27, 33). We note that the λ_{transp} values given in some studies (e.g., ref. 32) are not comparable to our θ because they are a function of multiple, independent variables (*SI Appendix*). The low θ_k value determined here has profound implications for modeling leaf water, particularly in arid environments. Previous modeling attempts were unable to match the low $\Delta'^{17}O$ values of animals from arid environments using assumed θ_k values of 0.518 (22, 26). Low $\Delta'^{17}O$ values measured in desert plants cannot be modeled unless our low θ_k value is used (*SI Appendix*). The new θ_k value better explains the low $\Delta'^{17}O$ values of plants from arid environments, and by extension, coexisting animals, ultimately allowing for better paleoclimate reconstructions to be made using fossil material.

Phytoliths. Phytoliths are accretions of solid hydrated opaline silica (silicon dioxide, $SiO_2 \bullet nH_2O$) that are deposited in the tissues of some plants, including horsetails and grasses. Studies suggest that the $\delta^{18}O$ values of phytoliths are directly related to the leaf water value and therefore indirectly provide an estimate of relative humidity during plant growth (23, 34–36). We analyzed coexisting phytoliths and leaf water along the length of an *Equisetum* stem (Fig. 3). The $1000ln^{18}\alpha_{silica\text{-}water}$ value of 35.89‰ for the lowest segment corresponds to a reasonable formation temperatures of 26 °C using a quartz–water fractionation equation (37). Moving up the stem, the fractionations decrease dramatically (Fig. 4). The upper part of the stem has a $1000ln^{18}\alpha$ value of only 10.3‰, clearly out of equilibrium. The regular $1000ln^{18}O\alpha$ decrease with height is explained by the continuous deposition of silica as the stem grows and elongates. At the beginning of the growing season, the upper segments are only a few cm above the ground surface, and the leaf water isotope value is low, similar to that of the soil water. The phytolith deposition at this stage would be in equilibrium with this light water. However, as the stem elongates, the upper segments attain increasingly higher leaf water isotope values and the developing phytoliths have correspondingly higher isotope values. The *integrated* triple oxygen isotope value of the phytolith carries both the isotopically light early growth and the extremely heavy overgrowth, resulting in integrated values that are between the two extremes. The example of the *Equisetum* phytoliths is extreme but clearly illustrates that equilibrium between xylem water and phytoliths is rarely or never attained. Nevertheless, there are clear relationships between relative humidity and the triple oxygen isotope values of phytoliths that can be used qualitatively to constrain relative humidity (35, 36).

Our phytolith triple isotope data along with previously published values are shown in Fig. 5. The data define a trend that does not go through the equilibrium triple oxygen isotope value for quartz–water fractionation. The $1000ln^{18}O\alpha_{phytolith\text{-}water}$ values for the lowest segment measured in our study match the

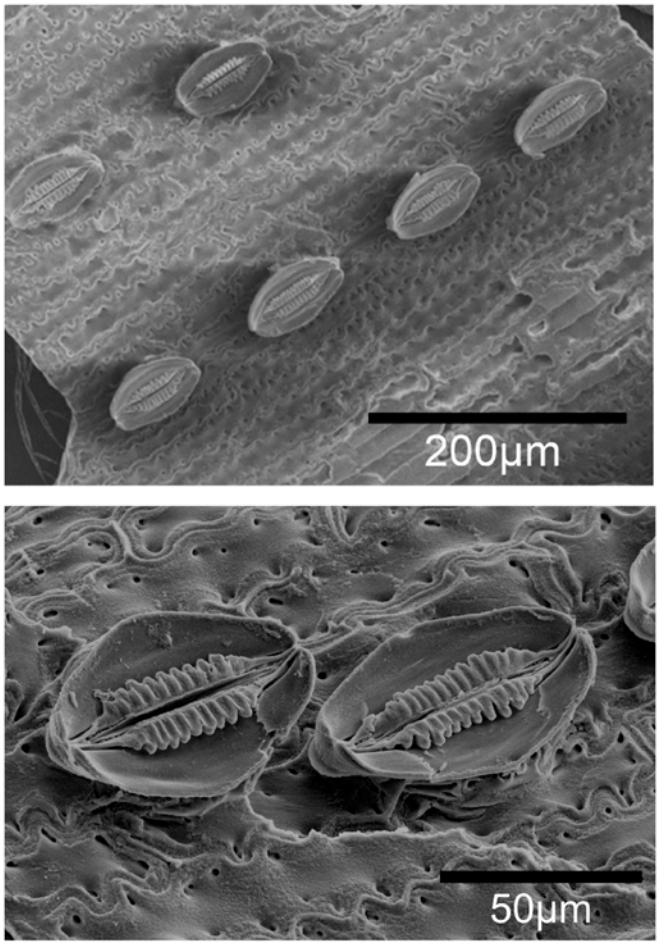

Fig. 3. Secondary electron microscopy (SEM) images of the inner epidermal surface in our *E. laevigatum* samples. The stomata are clearly visible in parallel rows, showing prominent silicified thickenings in the subsidiary cells.

quartz–water $\delta^{18}O$ fractionation but fall below the equilibrium $1000ln^{17}O(\alpha_{phytolith\text{-}water})$ value given by $\theta_{silica\text{-}water} = 0.524$ at 25 °C (37). Dodd et al. (38, 39) have shown that silica diatom frustules form out of equilibrium with ambient water. If we assume a similar kinetic fractionation for phytoliths, then agreement is attained with a θ value of 0.5205, similar to other published kinetic isotope fractionation factors (e.g., refs. 22 and 40).

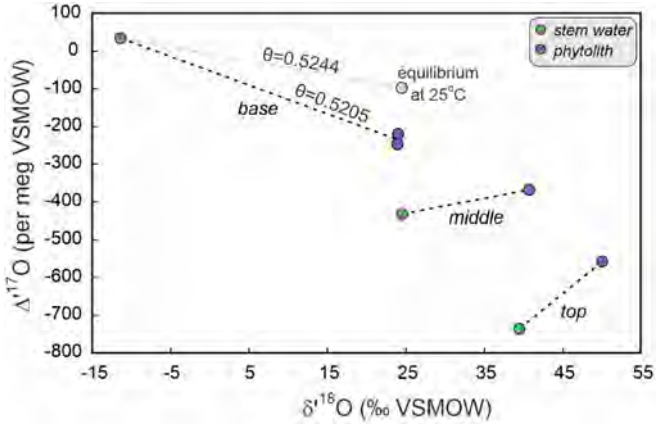

Fig. 4. Triple isotope composition of paired phytolith silica and corresponding stem water. The lowermost segment appears to be in isotopic equilibrium based on the $\delta^{18}O$ values alone but clearly shows a kinetic isotope effect when $\Delta'^{17}O$ values are included. Upper segments have an integrated isotope value attained over the course of the plant's growth.

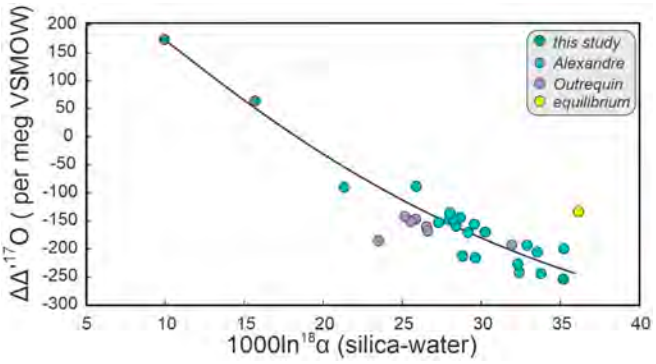

Fig. 5. Triple oxygen isotope fractionation between phytolith and stem water. The data plot on a smooth curve related to the integrated silica isotope composition and do not pass through the equilibrium silica–water fractionation at 25°C (yellow circle) demonstrating a kinetic effect. Data from this study and (23, 36). $\Delta\Delta'^{17}O$ (per meg) is equivalent to $\Delta'^{17}O_{silica} - \Delta'^{17}O_{water}$.

Discussion

The extreme oxygen isotope composition of *Equisetum* is related to the stagnant environment in the air spaces in the plant, which amplify the diffusional isotope effect (22). Linear enrichment is greater in *Equisetum* relative to *Poaceae* grass (9), likely related to slower water transport along the *Equisetum* stem. Overall, our data can be modeled using a leaf transpiration equation (7) with chain-of-lakes transport included. In *Equisetum*, the $\delta^{18}O$ values are the highest, and the $\Delta'^{17}O$ values lowest of any known materials on Earth, exclusive of stratospheric gases produced by mass independent ultraviolet photolysis (41). To illustrate the extreme values, Fig. 6 shows a compilation of previous triple-isotope data for all Earth materials and *Equisetum*. The *Equisetum* data are such outliers that, on the basis of the $\Delta'^{17}O$ values alone, one would reasonably conclude that this sample is of an extraterrestrial origin. The $\delta^{18}O$ values are far higher than any material from our Solar System (exclusive of extra-solar grains).

In contrast to the xylem water, *Equisetum* phytoliths do not show the same extreme isotopic enrichment as the stem water because silica deposition occurs over an extended period of time as segments expand. At an early growth stage (when the aerial stem is short and close to the ground), xylem water has far lower $\delta^{18}O$ and higher $\Delta'^{17}O$ values compared to later stages, when the aerial stem has elongated and xylem water has much higher $\delta^{18}O$ and lower $\Delta'^{17}O$ values. High spatial resolution isotope analyses of phytoliths should resolve the large variations expected to be preserved within a single phytolith.

Our approach could be applied to many other taxa known to have both high silica contents, spanning land-plant groups from ferns to angiosperms (43–46), and similar structures that would lead to evaporative oxygen isotope enrichment along photosynthetic and transpiring tissues. It is the loss of water from stems along the entire length of an *Equisetum* plant that results in the extreme $\delta^{18}O$ and $\Delta'^{17}O$ values. Low conductance for water from transpiring stems and vascular constraints between segments accentuate this effect (12, 15, 19). It is likely that a similar, though less extreme, isotope fractionation occurs in other plant groups (7). For example, among the closest living relatives of *Equisetum* are the ferns (e.g., ref. 47), which are also high silica accumulators.

Plant taxa that have long linear leaves and/or photosynthetic stems, such as commelinid monocots (e.g., palms, grasses, bananas) and some ferns (e.g., Pteridaceae), which also contain silica deposits (48), are also expected to experience oxygen isotopic enrichment along the length of an evaporating leaf, needle, or stem. This is especially so in

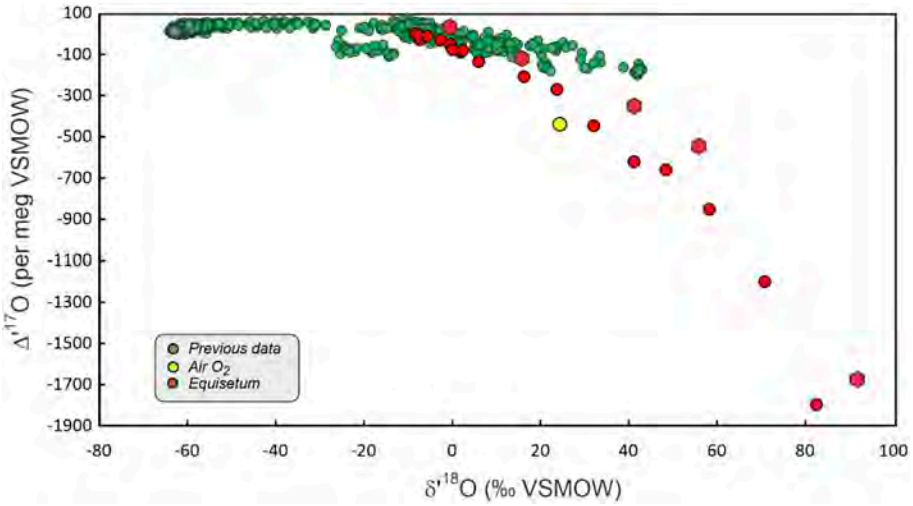

Fig. 6. Plot of published triple isotope data for terrestrial materials (20, 23), air O_2 (42), and *Equisetum* (this work). Two *Equisetum* isotope profiles are shown (circles and hexagons) and have similar trends. The *Equisetum* stem water $\delta^{18}O$ values are higher than any other measured samples from within our Solar System.

monocots where Helliker and Ehleringer (7) established that in grasses a similar progressive leaf water $\delta^{18}O$ enrichment exceeding 30‰ occurred along the length of a grass blade and that an equivalent $\delta^{18}O$ enrichment was also recorded in cellulose. While silica bodies were not measured in their studies, we would expect a similar axial oxygen isotope enrichment in grasses as well. Paleoclimate applications to fossil phytoliths should be used with caution, recognizing that the measured $\delta^{18}O$ values of phytoliths are a time-integrated average and that the water within a leaf or stem may be extremely modified from the local precipitation values.

Our results demonstrate that simple leaf water models may not adequately explain the range of $\Delta'^{17}O$ values found in some plants unless a chain-of-lakes model is included. Published fractionation equations for body water and leaf water clearly underestimate the magnitude of kinetic isotope effects in some cases. The effect is particularly apparent in plants and animals from arid environments where evaporation leads to extreme fractionation (*SI Appendix*, Fig. S5). The data can only be modeled using a θ_k value of 0.511, far lower than the generally accepted value of 0.518. The use of triple oxygen isotope data on fossil animal remains must consider the appropriate θ values when used for paleoclimate applications.

Materials and Methods

Equisetum stem segments were separated on site in the field and immediately placed in rubber-septum vacutainers. They were returned to the lab and kept in a constant temperature block at 25 °C to allow the stem water and newly formed CO_2 to equilibrate. After 24 to 48 h, CO_2 was quantitatively extracted by passing ultrapure He through the vacutainers for 5 min. The CO_2 was passed through a cold trap held at -80°C to remove traces of water and collected on a four-way valve cooled with liquid nitrogen. The CO_2 was admitted into a mixing line where the sample was diluted to 450 ± 2 ppm CO_2 with dry N_2 gas and measured on a tunable infrared laser direct absorption spectroscopy (TILDAS) system (see ref. 49 for details). Sample gas was alternated with a tank CO_2/N_2 reference gas with an isotope composition calibrated to VSMOW2-SLAP 2 scale (49). The $\alpha^{17}O_{(CO2\text{-}water)}$ value for our CO_2-water equilibrations was determined by measuring VSMOW2 and SLAP2 and found to be 1.0212. 12 alternating measurements were made of reference and sample gas. Analytical precision for $\delta^{18}O$ and $\Delta'^{17}O$ values are ±0.15‰ and ±10 per meg, respectively. In order to test the equilibration method, several segments of *Equisetum* were split longwise, with one half being equilibrated in a vacutainer as above and the second cryodistilled to quantitatively remove all water vapor. The extracted water was transferred to a vacutainer and 0.7 mL (STP) of CO_2 was injected into the vacutainer to equilibrate with the H_2O. Samples were allowed to equilibrate for 24 h at 25 °C. Both samples were measured using the same conditions on the TILDAS and found to be identical within analytical precision.

Phytoliths were isolated from plant tissues through wet chemistry oxidation procedures modified from ref. 34. Dry *Equisetum* stems were first reacted with 1M HCl for 30 min for carbonate removal and then rinsed with DI water three times. Subsequently, 99% sulfuric acid was added, and samples were placed on a hot plate for 3 to 4 h to dissolve organic matter. The hot plate was turned off, and the reaction was allowed to proceed overnight at room temperature. After ~10 h of reaction, 30% H_2O_2 was added to each sample to react all dissolved organic matter until the solution became clear. The samples were then vacuum filtered and rinsed with DI water. The filter was placed in a 60 °C drying oven overnight. Purified phytoliths were transferred to a small container and stored until analyzed. Purified samples were imaged in Tescan Vega 3 Scanning Electron Microscope with no noticeable organic contaminants observed.

Triple oxygen isotope measurements were performed on a laser fluorination line (50). About 3 mg of phytoliths were loaded onto a nickel sample plate. Samples were loaded into a vacuum chamber on the fluorination line and allowed to pump down for 10 h. Samples were prefluorinated with BrF_5 at ambient temperature for 30 to 40 min to remove structural water (38). For analysis, samples were reacted with excess BrF_5 using a 60W CO_2 laser. After the reaction, O_2 was separated from excess BrF_5 and other byproducts through a series of cryogenic traps. Purified O_2 was consolidated on a 13× mol sieve, further purified in a stream of He through a gas chromatographic column, and collected in a Thermo MAT 253+ on another mol sieve trap. Sample gas was analyzed 30 times using 28 s integration in dual inlet mode against an inhouse O_2 reference gas calibrated to VSMOW2-SLAP2 (51). Precision is 0.15‰ for $\delta^{18}O$ and 5 per meg for $\Delta'^{17}O$.

High-resolution Secondary Electron (SEM) images of selected carbon-coated phytoliths were taken with University of New Mexico's FEI Helios NanoLab 650 Dualbeam® Secondary Electron Microscope/Focused Ion Beam operating at 5 kV in high vacuum mode with a beam current of 0.10 nA.

Data, Materials, and Software Availability. All study data are included in the article and/or *SI Appendix*.

ACKNOWLEDGMENTS. All isotope measurements were made at the Center for Stable Isotopes, University of New Mexico. The project was conceived and partially executed as the ISOCAMP project for 14 students. ISOCAMP is a summer integrated lab-field class for stable isotopes (https://isocamp.org/). Partial funding for analyses was provided by ISOCAMP. Electron microscopy and sample preparation were carried out in the Nanomaterials Characterization Facility at the University of New Mexico, a facility that is supported by the State of New Mexico, the NSF and the NASA. Thanks to Jordan Anderson, Stephan Räss, and Elizabeth McGuire for their help during ISOCAMP.

Author affiliations: [a]Department of Earth and Planetary Sciences, University of New Mexico, Albuquerque, NM 87122; [b]Earth and Planetary Sciences, Yale University, New Haven, CT 06511; [c]Lunar and Planetary Institute, Houston, TX 77058; [d]Department of Archaeology, University of Cape Town, Rondebosch 7701, South Africa; [e]Geology and Geophysics, University of Utah, Salt Lake City, UT 84112; [f]School of Biological Sciences, University of Utah, Salt Lake City, UT 84112; [g]University of California Santa Cruz Stable Isotope Lab, University of California Santa Cruz, Santa Cruz, CA 95064; [h]Department of Biology, University of Washington, Seattle, WA 98195-1800; [i]Department of Forest Ecology and Management, Swedish University of Agricultural Sciences, Umeå 901 83, Sweden; [j]Earth and Atmospheric Sciences, University of Alberta, Edmonton, AB T6G 2E9, Canada; [k]Department of Oceanography, University of Hawaii at Mānoa, Honolulu, HI 96822; [l]Department of Earth System Science, University of California at Irvine, Irvine, CA 92697-310; [m]Department of Geological Sciences, The University of Alabama, Tuscaloosa, AL 35487-0338; [n]Department of Earth Sciences, University of Rome, Roma 00185, Italy; [o]Department of Anthropology, University of Oregon, Eugene, OR 97403-1245; [p]Department of Chemistry, SUNY College of Environmental Science and Forestry, Syracuse, NY 13210; [q]Centre for Research and Teaching in Environmental Geoscience, French National Centre for Scientific Research, Aix-en-Provence 13545, France; [r]Department of Earth, Environmental, and Planetary Sciences, Brown University, Providence, RI 02912; and [s]Royal Botanic Gardens, Kew, Richmond, Surrey TW9 3AB, United Kingdom

1. S. Jasechko *et al.*, Terrestrial water fluxes dominated by transpiration. *Nature* **496**, 347–350 (2013).
2. J. R. Ehleringer, T. E. Dawson, Water uptake by plants: Perspectives from stable isotope composition. *Plant Cell Environ.* **15**, 1073–1082 (1992).
3. G. D. Farquhar, L. A. Cernusak, B. Barnes, Heavy water fractionation during transpiration. *Plant Physiol.* **143**, 11–18 (2007).
4. L. B. Flanagan, J. P. Comstock, J. R. Ehleringer, Comparison of modeled and observed environmental influences on the stable oxygen and hydrogen isotope composition of leaf water in *Phaseolus vulgaris* L. *Plant Physiol.* **96**, 588–596 (1991).
5. J. S. Roden, J. R. Ehleringer, Observations of hydrogen and oxygen isotopes in leaf water confirm the Craig-Gordon model under wide-ranging environmental conditions. *Plant Physiol.* **120**, 1165–1173 (1999).
6. S. A. Kannenberg, R. P. Fiorella, W. R. L. Anderegg, R. K. Monson, J. R. Ehleringer, Seasonal and diurnal trends in progressive isotope enrichment along needles in two pine species. *Plant Cell Environ.* **44**, 143–155 (2021).
7. B. R. Helliker, J. R. Ehleringer, Establishing a grassland signature in veins: ^{18}O in the leaf water of C_3 and C_4 grasses. *Proc. Natl. Acad. Sci. U.S.A.* **97**, 7894–7898 (2000).
8. G. Dongmann, H. W. Nürnberg, H. Förstel, K. Wagener, On the enrichment of $H_2{}^{18}O$ in the leaves of transpiring plants. *Radiat. Environ. Biophys.* **11**, 41–52 (1974).
9. B. R. Helliker, J. R. Ehleringer, Grass blades as tree rings: Environmentally induced changes in the oxygen isotope ratio of cellulose along the length of grass blades. *New Phytol.* **155**, 417–424 (2002).
10. B. R. Helliker, J. R. Ehleringer, Differential ^{18}O enrichment of leaf cellulose in C_3 versus C_4 grasses. *Funct. Plant Biol.* **29**, 435–442 (2002).
11. M. Wachtler, "The Middle devonian flora explosion" in *The Middle Devonian Flora Explosion–The Origins of Higher Plants*, M. Wachtler, N. Wachtler, Eds. (Dolomythos-Museum, 2023), pp. 17–72.
12. C. Husby, Biology and functional ecology of *Equisetum* with emphasis on the giant horsetails. *Bot. Rev.* **79**, 147–177 (2013).
13. Z. Feng, T. Zierold, R. Rößler, When horsetails became giants. *Chin. Sci. Bull.* **57**, 2285–2288 (2012).
14. A. Knowlton, *Equisetum*. *Curr. Biol.* **22**, R388–R390 (2012).
15. C. E. Husby, *Ecophysiology and Biomechanics of Equisetum giganteum in South America* (Florida International University, Miami, 2009), p. 182.
16. E. Cullen, P. J. Rudall, The remarkable stomata of horsetails (*Equisetum*): Patterning, ultrastructure and development. *Ann. Bot.* **118**, 207–218 (2016).
17. D. M. Sytnikov, G. V. Kucherik, Structure and physiological state of field horsetail tissues. *Ekosistemy* **30**, 64–68 (2022).
18. A. M. F. Tomescu, I. H. Escapa, G. W. Rothwell, A. Elgorriaga, N. R. Cúneo, Developmental programmes in the evolution of *Equisetum* reproductive morphology: A hierarchical modularity hypothesis. *Ann. Bot.* **119**, 489–505 (2017).
19. C. E. Husby, J. Delatorre-Herrera, S. A. Oberbauer, A. Grau, L. Novaro, Stomatal conductance patterns of *Equisetum* giganteum stems in response to environmental factors in South America. *Botany* **92**, 701–712 (2014).
20. Z. D. Sharp, J. A. G. Wostbrock, A. Pack, Mass-dependent triple oxygen isotope variations in terrestrial materials. *Geochem. Perspect. Lett.* **7**, 27–31 (2018).
21. P. G. Aron, S. Li, J. R. Brooks, J. M. Welker, N. E. Levin, Seasonal variations in triple oxygen isotope ratios of precipitation in the Western and Central United States. *Paleoceanogr. Paleoclimatol.* **38**, e2022PA004458 (2023).
22. B. H. Passey, N. E. Levin, Triple oxygen isotopes in meteoric waters, carbonates, and biological apatites: Implications for continental paleoclimate reconstruction. *Rev. Mineral. Geochem.* **86**, 429–462 (2021).
23. A. Alexandre *et al.*, The triple oxygen isotope composition of phytoliths as a proxy of continental atmospheric humidity: Insights from climate chamber and climate transect calibrations. *Biogeosciences* **15**, 3223–3241 (2018).
24. E. Barkan, B. Luz, High precision measurements of $^{17}O/^{16}O$ and $^{18}O/^{16}O$ ratios in H_2O. *Rapid Commun. Mass Spectrom.* **19**, 3737–3742 (2005).
25. L. Merlivat, Molecular diffusivities of H_216O, $HD^{16}O$, and $H_2{}^{18}O$ in gases. *J. Chem. Phys.* **69**, 2864–2871 (1978).
26. E. Barkan, B. Luz, Diffusivity fractionations of $H_2{}^{16}O/H_2{}^{17}O$ and $H_2{}^{16}O/H_2{}^{18}O$ in air and their implications for isotope hydrology. *Rapid Commun. Mass Spectrom.* **21**, 2999–3005 (2007).
27. A. Pierchala, K. Rozanski, M. Dulinski, Z. Gorczyca, Quantification the diffusion-induced fractionation of $^1H_2{}^{17}O$ isotopologue in air accompanying the process of water evaporation. *Geochim. Cosmochim. Acta* **322**, 244–259 (2022).
28. G. D. Farquhar, J. Lloyd, "Carbon and oxygen isotope effects in the exchange of carbon dioxide between terrestrial plants and the atmosphere" in *Stable Isotopes and Plant Carbon-Water Relations*, J. R. Ehleringer, A. E. Hall, G. D. Farquhar, Eds. (Academic Press, San Diego, 1993), pp. 47–70.
29. J. R. Gat, Oxygen and hydrogen isotopes in the hydrologic cycle. *Annu. Rev. Earth Planet. Sci.* **24**, 225–262 (1996).
30. J. J. Gibson, S. J. Birks, Y. Yi, Stable isotope mass balance of lakes: A contemporary perspective. *Quat. Sci. Rev.* **131**, 316–328 (2016).
31. V. J. Hare *et al.*, Triple oxygen isotopes in eggshell carbonate as a proxy of late Cenozoic CO_2 and primary productivity. *Geochim. Cosmochim. Acta* **399**, 48–63 (2025).
32. A. Landais, E. Barkan, D. Yakir, B. Luz, The triple isotopic composition of oxygen in leaf water. *Geochim. Cosmochim. Acta* **70**, 4105–4115 (2006).
33. A. Angert, C. D. Cappa, D. J. DePaolo, Kinetic ^{17}O effects in the hydrologic cycle: Indirect evidence and implications. *Geochim. Cosmochim. Acta* **68**, 3487–3495 (2004).
34. E. A. Webb, F. J. Longstaffe, The oxygen isotopic compositions of silica phytoliths and plant water in grasses: Implications for the study of paleoclimate. *Geochim. Cosmochim. Acta* **64**, 767–780 (2000).
35. C. Voigt *et al.*, Examination of the parameters controlling the triple oxygen isotope composition of grass leaf water and phytoliths at a Mediterranean site: A model–data approach. *Biogeosciences* **20**, 2161–2187 (2023).
36. C. Outrequin *et al.*, The triple oxygen isotope composition of phytoliths, a new proxy of atmospheric relative humidity: Controls of soil water isotope composition, temperature, CO2 concentration and relative humidity. *Clim. Past* **17**, 1881–1902 (2021).
37. Z. D. Sharp *et al.*, A calibration of the triple oxygen isotope fractionation in the SiO_2–H_2O system and applications to natural samples. *Geochim. Cosmochim. Acta* **186**, 105–119 (2016).
38. J. P. Dodd, Z. D. Sharp, A laser fluorination method for oxygen isotope analysis of biogenic silica and a new oxygen isotope calibration of modern diatoms in freshwater environments. *Geochim. Cosmochim. Acta* **74**, 1381–1390 (2010).
39. J. P. Dodd, Z. D. Sharp, P. J. Fawcett, A. J. Brearley, F. M. McCubbin, Rapid post-mortem maturation of diatom silica oxygen isotope values. *Geochem. Geophys. Geosyst.* **13**, Q09014 (2012).
40. W. Guo, C. Zhou, Patterns and controls of disequilibrium isotope effects in speleothems: Insights from an isotope-enabled diffusion–reaction model and implications for quantitative thermometry. *Geochim. Cosmochim. Acta* **267**, 196–226 (2019).
41. M. H. Thiemens, History and application of mass-independent isotope effects. *Annu. Rev. Earth Planet. Sci.* **34**, 217–262 (2006).
42. Z. D. Sharp, J. A. G. Wostbrock, "Standardization for the triple oxygen isotope system: Waters, silicates, carbonates, air, and sulfates" in *Reviews in Mineralogy and Geochemistry*, I. Bindeman, A. Pack, Eds. (Mineralogical Society of America, 2021), vol. 86, pp. 179–196.
43. R. Sharma, V. Kumar, R. Kumar, Distribution of phytoliths in plants: A review. *Geol. Ecol. Landscapes* **3**, 123–148 (2019).
44. M. J. Hodson, P. J. White, A. Mead, M. R. Broadley, Phylogenetic variation in the silicon composition of plants. *Ann. Bot.* **96**, 1027–1046 (2005).
45. M. Sundue, Silica bodies and their systematic implications in Preridaceae (Pteridophyta). *Bot. J. Linn. Soc.* **161**, 422–435 (2009).
46. C. J. Prychid, P. J. Rudall, M. Gregory, Systematics and biology of silica bodies in monocotyledons. *Bot. Rev.* **69**, 377–440 (2004).
47. B. D. Ruhfel, M. A. Gitzendanner, P. S. Soltis, D. E. Soltis, J. G. Burleigh, From algae to angiosperms–Inferring the phylogeny of green plants (Viridiplantae) from 360 plastid genomes. *BMC Evol. Biol.* **14**, 14–23 (2014).
48. P. J. Rudall, J. Lourenco, M. Kumar-Mahto, Biosilicification in monocots: Comparative analysis highlights contrasting patterns of deposition. *Am. J. Bot.* **112**, e70074 (2025).
49. N. Perdue, Z. Sharp, D. Nelson, R. Wehr, C. Dyroff, A rapid high-precision analytical method for triple oxygen isotope analysis of CO2 gas using tunable infrared laser direct absorption spectroscopy. *Rapid Commun. Mass Spectrom.* **36**, e9391 (2022).
50. Z. D. Sharp, A laser-based microanalytical method for the in situ determination of oxygen isotope ratios of silicates and oxides. *Geochim. Cosmochim. Acta* **54**, 1353–1357 (1990).
51. J. A. G. Wostbrock, E. J. Cano, Z. D. Sharp, An internally consistent triple oxygen isotope calibration of standards for silicates, carbonates and air relative to VSMOW2 and SLAP2. *Chem. Geol.* **533**, 119432 (2020).